

SLOWLY ROTATING 3D FIELD FOR LOCKED MODE AVOIDANCE AND H-MODE RECOVERY IN DIII-D

M. OKABAYASHI
Princeton Plasma Physics Laboratory
Princeton, NJ USA
Enmail:mokabaya@pppl.gov

L. SUGIYAMA
Massachusetts Institute of Technology
Cambridge,
MA USA

D.P. BRENNAN
Princeton Plasma Physics Laboratory
Princeton, NJ USA

S. INOUE
National Institutes for Quantum and Radiological Science and Technology
Tokai, Ibaraki Japan

C. CHRYSTAL, R.J. LA HAYE, E.J. STRAIT
General Atomics
San Diego, CA USA

M. AUSTIN
University of Texas
Austin, TX USA

N.C. LOGAN, C. HOLCOMB, B. VICTOR
Lawrence Livermore National Laboratory,
Livermore, CA USA

J. HANSON
Columbia University
New York, NY USA

Abstract

A slowly rotating 3D field has been considered a promising approach for preventing the locking and growth of NTM-driven disruptions in high beta plasmas, or enhancing the H-mode recovery. Recently, M3D [1], numerical simulations have found new properties of the $q=1$ modes in these plasmas that suggest the possibility of using the rotating 3D field to sustain the plasma core against quasi-interchange (QI)-driven sawtooth crashes, at the same time as avoiding NTMs locking at $q>1$. The characteristic $q\sim 1$ QI modes are found to have dominant $n=1$ and 2 toroidal harmonics of comparable magnitude that are well suited to interact with the external 3D field. Preliminary experimental observations in hybrid configuration discharges support the possibility of quasi-interchange mode control with the slowly rotating 3D field and suggest that it can be explored simultaneously with the control of NTM locking avoidance.

1. INTRODUCTION

The high beta plasmas with slowly rotating 3D field have been explored as a promising approach for avoiding the locking of neoclassical tearing modes (NTMs) and improving H-mode recovery against NTM-driven disruptions. Recently, numerical MHD simulations of these plasmas using M3D simulation code [1,2] have revealed the external 3D field may have an additional advantage for the sustainment of the core in the quasi-interchange (QI) regime. This is based on the unique characteristics of the QI instability in these plasmas, namely multiple toroidal harmonics at the

lowest toroidal harmonic mode numbers $n=1$ and 2 with magnetic perturbations that extend well outside $q=1$ domain. This paper reports preliminary experimental observations in an ITER baseline scenario development discharge in DIII-D that support these simulation predictions. The experiments indicate that control of the quasi-interchange mode over $q \leq 1$ can be explored simultaneously with the locking avoidance of NTMs at $q > 1$, using the same slowly-rotating 3D field.

The paper first briefly summarizes MHD simulation results on QI modes with an applied rotating resonant

magnetic perturbation (RMP) DIII plasma using the M3D code [3] that are very useful to understand the experimental observations. The plasma configuration considered in this paper is the hybrid plasma with the central safety factor $q(0)$ just above unity. We show the 3D field of the I-coil that was applied for the $m/n = 2/1$ (m is the poloidal harmonic) NTM locked-mode avoidance can also contribute to regulating the QI mode instability by controlling the core Te collapse, consistent with the suggestion by the numerical simulation. The preliminary experimental observations include several elements. The core Te collapse deforms the plasma column in a helical manner. The experimental analysis confirms the existence of internal $n=1$ and $n=2$ harmonics. The phasing control between the applied 3D field and the instantaneous plasma response through feedback [4, 5] indicates that it is possible to control the couplings between the $n=1$ and $n=2$ harmonics. The reduction of coupling between internal $n=1$ and $n=2$ harmonics may make it simpler to stabilize NTMs in hybrid configurations.

Disruptions due to the locking and growth of neoclassical tearing modes are one of potential obstacles remaining for successful tokamak-based fusion burning in ITER and beyond. The external application of a slowly rotating $n=1$ RMP could stabilize the most dangerous tearing-locking at $q > 1$, in particular the $2/1$ mode at $q=2$. New results show a possibility that the rotating RMP also produces general plasma conditions favorable for central fusion burning, through a unique set of effects. Small sawteeth driven by QI-modes (here called QI-driven crash) are much more favorable for fusion burning than the larger amplitude internal kink-driven sawteeth at $q(0) < 1$.

2. QUASI INTERCHANGE INSTABILITY AND QUASI-STEADY STATE

Numerical simulation with the extended MHD code M3D[1,2] was carried out for the DIII-D ITER-baseline plasma shape discharge with $q(0) \sim 1$ and $q_{95} \sim 4.0$ (#166564 at $t=3445$ ms), when an $n=1$ rotating RMP was applied to prevent the rotational locking of the $2/1$ NTM[3]. It showed that the central low magnetic shear $q \lesssim 1$ region is unstable to a nearly ideal quasi-interchange (QI) mode that causes a sawtooth-type crash. The simulation used the experimental profiles and parameters of discharge after the original $2/1$ NTM at $q=2$ had been successfully suppressed by the applied RMP. The RMP itself was not included, due to its very slow rotation frequency.

The simulation followed the QI instability from very small amplitude to its maximum growth rate and the central QI-driven crash that flattened the core profiles of temperature T and the toroidal current density J_ϕ , followed by profile healing and eventual establishment of a perturbed quasi-steady QI state over $q \approx 1$. Figure 1 shows the details, taken from the case of Ref. [3]. Due to the low magnetic shear, the QI modes in the initial stages of the crash are fundamentally nonlinear, characterized by two toroidal numbers $n=1$ and 2 of comparable magnitude that grow at the same rate (Fig.1(b,c)). At low amplitude, these are $1/1$ and $2/2$ inside $q=1$, respectively. The sawtooth-like crash, shown by the temperature profile evolution in Fig.1(a), resemble experimentally observed QI-driven crash in DIII-D 153967 (as shown in Section 3.1), which differs from the resistive internal kink.

The QI crash is dominated by smooth interchange flows transverse to the magnetic field. The simulated mode initially has $n=1$ and 2 , but becomes strongly $n=1$ at the height of the crash (Fig.1 (b,c)). The interchange flows determine the plasma and magnetic field motion. The flows steadily displace the hotter plasma core and separate its contact region with the $q=1$ surface in two halves. The two contact regions continue to narrow poloidally, until a strong localized interchange process expels the remaining core pressure out to a mixing radius well outside the $q=1$ (see Fig. 11 in Ref. [3]). There are no resonant X-points or large-scale magnetic reconnection at $q=1$. The final expulsion is strongly $n=1$. Because the entire central q region remains close to unity, the perturbed magnetic field $|\delta B|$ remains small. After the crash heals, a quasi-steady state develops, with sustained strong $n=1$ and $n=2$ harmonics inside the low shear $q \approx 1$ region and a hollow axisymmetric temperature profile. Many of the QI mode properties predicted in the simulation [3], including the stability analysis, are seen in the actual plasma 166564 and in the discharges discussed in this paper.

The existence of the large $n=2$ harmonic in the simulated $q=1$ QI mode at low amplitude, and its higher $m=n+1$ sidebands that extend well outside $q=1$, suggest that the $n=2$ harmonics of the rotating RMP might be used for MHD control of the QI driven-crash, while the $n=1$ RMP harmonic were used to suppress the $2/1$ NTM (Dual $n=1$ & $n=2$ combined system). Control using $n=2$ is unlikely to be possible for the conventional resistive internal kink sawtooth, because it is $n=1$ until shortly before the final crash. Preliminary discussion of $n=2$ involvement in the control experiment is reported in this paper.

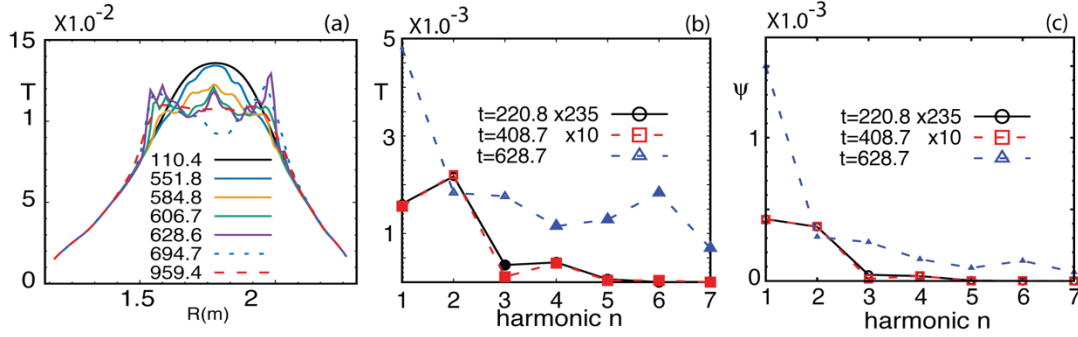


Fig.1. Simulated $q=1$ QI crash in 166564. (a) Midplane MHD temperature profiles over the crash, for a toroidal angle $\phi=96$ degrees where the mode moves vertically upward off the midplane (code units, times in τ_A). Toroidal spectra $n=1-7$ of the perturbed (b) poloidal magnetic field $\tilde{\psi}$ and (c) temperature \tilde{T} , for the low amplitude QI mode at early times $t=220$ (black, scaled by a factor 235x) and 408 (red, scaled by 10x), compared to the fast crash $t=628.4$ when $n=1$ becomes dominant.

3. EXPERIMENTAL OBSERVATIONS

Figure 2 shows an example of how the NTM behaves around $\beta_N \sim 3$ in hybrid configuration with $q(0)$ nearly unity and the H-mode recovery[6]. In this shot, H-mode was formed just after the initial plasma current ramp-up around $t=1600$ ms (not shown). The edge pedestals of electron temperature T_e and density n_e profiles were kept in a steady manner over a few hundred milliseconds. In this shot, the onset of NTM which unexpectedly caused the massive gas inflow (seen in the burst in saturated $D\alpha$ signal at $t \sim 1980$ ms) inducing a fast T_e pedestal decay and loss of the H-mode. The magnetic sensor signal monitoring the NTM amplitude and growth rate activated the application of 3D field. The general concern is that if the NTM grows too large, it may be impossible for a $n=1$ only system to control the mode locking. Just after the L-mode began, the preprogrammed frequency began at 20 Hz and quickly increased in time with the rate of 100Hz over 100ms. At the H-mode recovery time, the frequency was around 50Hz[6]. The magnetic sensor signal shows the MHD mode was synchronized with the RMP I-coil current and did not lock to the wall. The plasma condition was a typical hybrid scenario with $\beta_N \sim 2.1$, $q_{95} \sim 4.0$ and density $4.1 \times 10^{19} \text{ m}^{-3}$ when the coils locked the mode. The mode structure and QI mode behavior was monitored with the Electron Cyclotron Emission (ECE) signal.

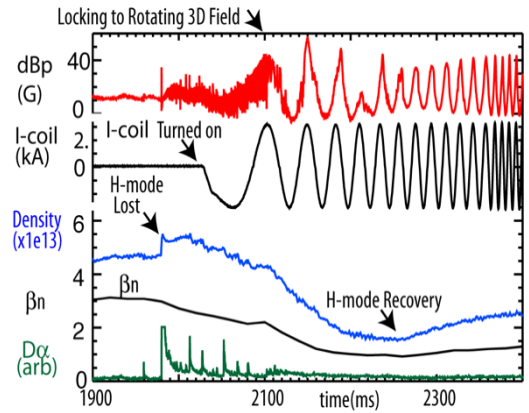


Fig. 2. The discharge development around the H-mode onset (#153967).

3.1. EXPERIMENTAL RESULTS

The time period of QI-driven crash around H-mode recovery is shown in Figure 3. The development of the QI-driven crash and T_e flattening evolution in time was illustrated by the perturbed electron temperature δT_e calculated from ECE T_e by subtracting the running average over one cycling period of 3D field around the time of interest. Although the critical QI-driven crash activity began around $t=2152$ ms, δT_e flattening by QI-activity started much earlier just after the main NTM started to synchronize with the applied 3D field around $t=2100$ ms. The partial QI-driven flattening was visible when the tearing mode (NTM) was locked to the applied 3D field around 2150ms.

Around that time period, the dominant oscillatory component of the NTM began to vanish away. With the 50Hz range of 3D field rotation, the main plasma began to show a response unified from the core to near the edge. This led to the initiation of a periodic QI-driven crash at every other cycle of I-coil current. The initial boundary behavior (around $\rho=0.2-0.3$) began to change from H-mode recovery around $t=2252\text{ms}$. The following crash ($t=2300\text{ms}$) was formed with two off-centered cool regions. With further recovery of the H-mode, the central crash is sharper around $t=2335\text{ms}$. The blue-colored area indicates a large sharp Te drop was taking place with longer recovery time. The QI-driven crash became regularly repetitive at every 3D Field cycle with a frequency of $\sim 150\text{ Hz}$ later in time (not shown). Next, using the reproducible time period, we look at the mode structure as the numerical simulation suggested.

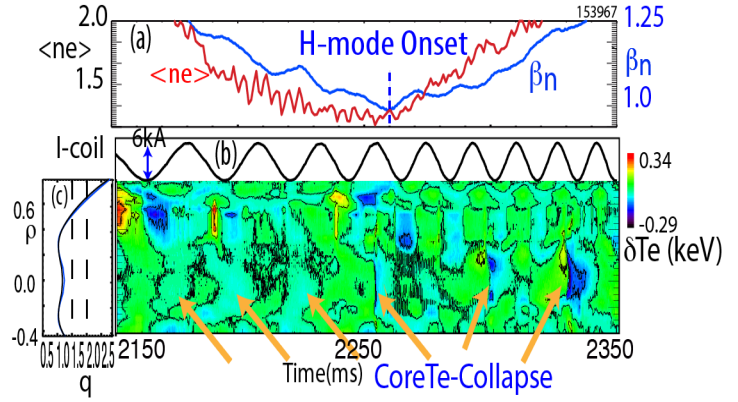


Fig. 3. The Core-Te-collapse behavior around H-mod onset (#153967)
(a) The electron density and beta-n, β_n ,
(b) I-coil current and the perturbed dTe
(c) the q -profile(x -axis) vs. ρ (y -axis)

Figure 4 shows the QI-driven crash with an RMP frequency of 120 Hz, about 150 ms after the onset of H-mode. The Thomson scattering shows a well-established Te and ne H-mode edge profile during this time (not shown). The details of the formation of Te collapse and perturbed Te profile were calculated from the ECE by subtracting the DC profile offset at $t=2480\text{ms}$ to minimize the uncertainty due to the possible Te profile rapid change during the crash event. The q -profile [Figure 4(a)] was obtained from the EFIT calculation with MSE Bz measurement but no kinetic correction included. The δTe behavior shown in the Figure 4(b) contour and the expanded contour (Figure 4(d)) shows two small radially-localized cool regions first appears off-axis: $\rho = 0.25$ in the Low Field Side (LFS) and $\rho = -0.25$ at the High Field Side (HFS). These two initial growing cool cells drift toward the axis in a manner of avalanche, of which time evolution is visible in Figure 4(d). The one initiated at LFS might have not propagated smoothly until it reached a little toward the core axis as shown in Figure 4(d). The plasma equilibrium may be slightly asymmetric so that the initial tiny crashes at HFS/LFS evolve differently until the penetration reached below $\rho = 0.2$. The two cool regions took a few hundred microseconds to reach the magnetic axis, producing a crescent-shaped cliff of a few hundred electron-volt drop on the ECE signals. The QI observation on the midplane such as mode structure (Fig. 4(e)) and its resulting to the crescent shape collapse in time is in a good agreement of the 3D simulation results of Fig.1 (a). The simulation [3] shows at the complete process takes place through the poloidal interchange flow mechanism without any resonant reconnection at $q=1$.

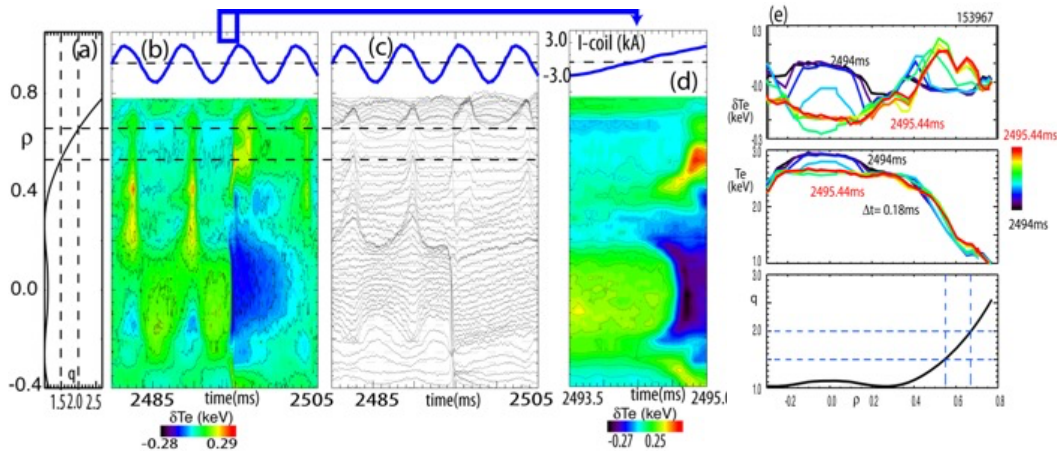


Fig.4. The formation of Te collapse. (a) q vs δ , (b) the δTe contour (c) the δTe vs time (d) the expanded Te collapse and (e) the δTe crash details and Te profile(top) and dTe (middle) vs ρ -radius at various time slices, $t=2594\text{ms}$ (blue), and $=2495.44\text{ms}$ (red) ms and with every $144\mu\text{s}$ interval), The blue curves in Fig.(b,c,d) are I-coil current and q vs. ρ (#153967).

This local Te profile drop by crash decays away with a 7-10ms decay time constant. These slow time-developments indicate that transport processes are involved in the setting-up condition and the onset of QI-driven collapse. It is also possible that the QI-mode itself influences the transport properties. Next, we look at the possible involvement of low- n components as the numerical simulation suggested using the reproducible time period.

3.2. THE RECONSTRUCTED MULTI-TOROIDAL COMPONENTS WITH MAGNETIC SENSORS

The information of radial perturbation toroidal wavenumber is highly desirable. However, the radial profile measurement is available at only one toroidal location. On the other hand, magnetic sensors are located at various toroidal angles outside the plasma and provide the amplitude and phase with sub-millisecond time resolution over multi-toroidal harmonics.

By assuming that the information from the internal events dominantly involved in the magnetic process is transmitted outward without additional dissipation to the plasma boundary, we can relate the magnetic sensor signals to the perturbed-profile components. Here, δTe from the ECE signals is decomposed as a sum over the lowest toroidal harmonics as

$$\delta T_{e,j} = \sum_{n=1,2,3} C_{n,j}(r,j) * \delta B_n(t)$$

The $\delta B_n(t)$ is expressed by complex components determined from magnetic sensor signal decomposition. The complex coefficient $C_{n,j}$ is determined by taking average over one cycling time period of 3D field with the error minimization each observation surface. Thus, the toroidal phase shift such as due to resistivity can be included by the complex coefficient radial profile. Reconstructed toroidal component is given by,

$$\delta T_{e,n,j.reconst}(r, t_{sampling}) = C_{n,j} * \delta B_n$$

The examples are shown in Figure 5 and 6 corresponding to the time period before the crash (2480-2493ms) as shown in Figure 4(a,b). We did not include the collapse dominated time period here, since the coefficient $C_{n,j}$ is assumed to be constant over each surface. Figure 4 (a) shows the I-coil current and the inputs to the analysis, namely the magnetic sensor signals of $n=1,2,3$. (I-coil current was not used for the calculation). The fitting results (blue curves) and the input ECE signals (black) are shown in Figure 5(b).

Figure 6 shows the reconstructed radial $\delta T_{n=1,j.reconst}$ profile at various time before the crash. The $n=1$ component of reconstructed $\delta T_{n=1,j.reconst}$ provides where rational surfaces may exist. The odd-parity behavior seen between $\rho=0.2$ and $\rho=-0.2$ at any time slices indicates these two locations are rational surfaces at $\rho=\pm 0.2$. The resonant response is also seen at $\rho=0.65$ corresponding to a 2/1 mode. The radius of $\rho=0.2$ or -0.2 could be attributed to a safety factor of unity. On the other hand, it is hard to explain the rational surface at $\rho=0.4$ with a monotonic q profile. Thus,

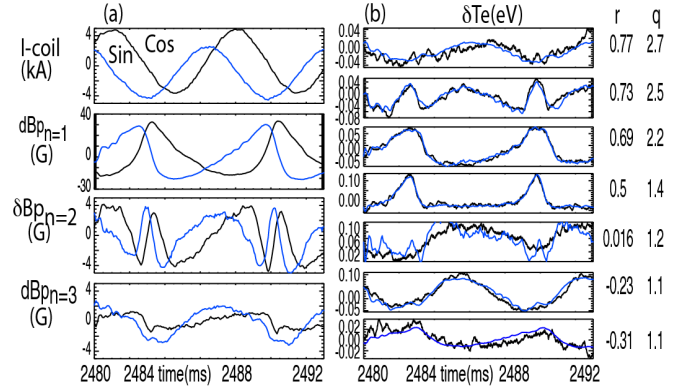


Fig. 5. The magnetic sensor input signals to determine the reconstructed δTe (#153967): (a) from the top, I-coil, $n=1$, $n=2, n=3$ components. (b) comparison of the fitting between the ECE signals (black) and the reconstructed δTe (blue)

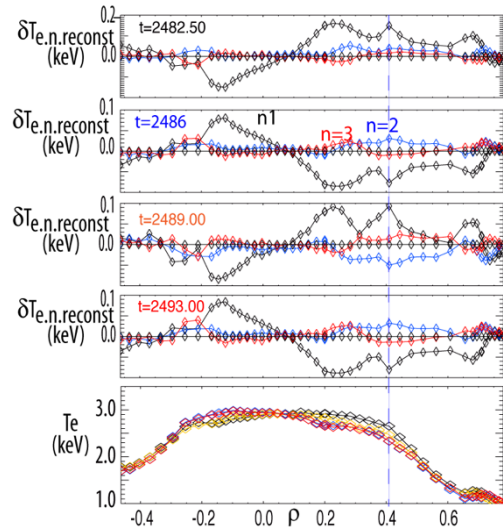


Fig. 6. The radial structure of $\delta T_{n.reconst}$ profiles of the components, $n=1$ (black), $n=2$ (Blue), $n=3$ (red). Time slices are 2482.50ms, 2486ms, 2489ms and 2493ms. The profile at the bottom are total components added at 2482.5ms (Black), 2486ms (Blue), 2489ms (Orange) and 2493ms (red)

tentatively, we assume that a second helical- q -unity surface exists in this configuration, as suggested by Figure 4(e). We will reexamine this assumption a-priori. The $n=2$ component of reconstructed $\delta T_{n=2,j.reconst}$ magnitude remains finite but show some indication of peaking at $r=0.4$.

4. QUASI INTERCHANGE MODE UNDER TEARING LOCKING AVOIDANCE CONTROL

The M3D simulation in Section 2 showed that the amplitude of the $n=1$ and $n=2$ components are comparable when the QI-driven crash grows and suggested that this was a general property of these DIII-D plasmas with low shear $q=1$ regions. The rotating $n=1$ RMP feedback fits well to the dual purpose of preventing the locking of the $2/1$ NTM and investigating the QI-driven crash. The feedback requests the adjustment of the I-coil current to have a finite phase delay relative to the observed mode component as if pushing the observed component behind. The feedback minimizes the phase between the 3D field and the mode excited in plasma. At the same time, the feedback also tries to reduce the amplitude of the observed mode.

Figure 7 shows the results of the 3D feedback control to unlock the NTM which was already locked earlier (~ 300 ms before). The preliminary survey before this shot had indicated that the plasma condition was very sensitive to the extra 3D field application. Thus, the DC component of I-coil current was gradually increased to a typical error field correction level of 1kA after the locking to the wall (the error field correction was provided separately by the C-coil system). Here, the AC frequency feedback range was set to around 30 Hz, which is a factor of five slower than the preprogrammed operation discussed in section 3. After the 3D field was applied initially as shown in Figure 7(b,d) at $t=2520$ ms, the relative phase difference at the maximum amplitude between the 3D field and $n=1$ mode (also $n=2$) became small. However, the mode amplitude was gradually increased. The better coupling between the 3D field and the plasma response is likely to have helped reduce the applied frequency. At same time, the core-collapse structure began to evolve in time. The balance of $n=1$ and $n=2$ components remains to be improved.

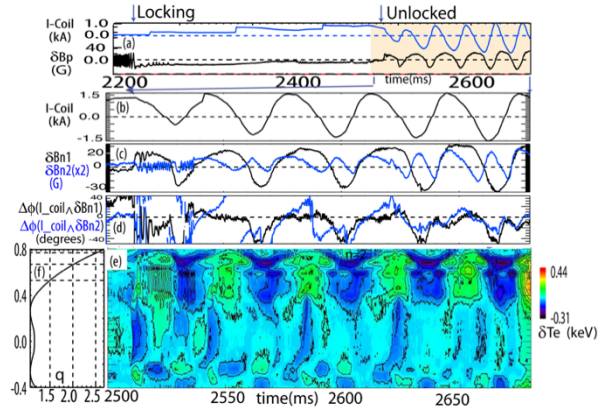


Fig. 7. QI mode under tearing mode locking avoidance: (a) I-coil current and magnetic signal, (b) I-coil current, and magnetic sensor signal amplitude with decomposition, $n=1$, $n=2(x2)$ (d) the phase difference between the external field and $n=1$ (black) and $n=2$ (blue) component, (e) the contour of dTe , and (f) ρ vs. q (#153974)

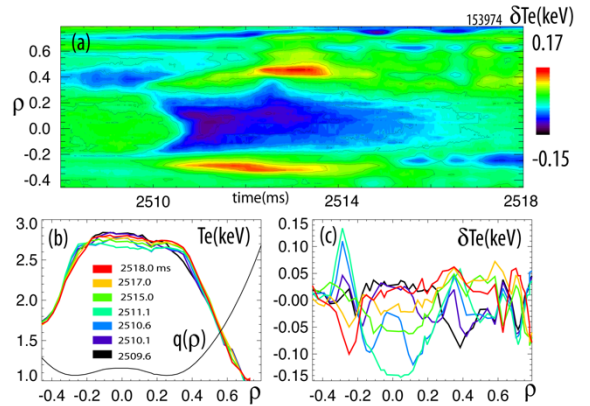


Fig. 8. The QI-crash structure at $t=2510$ ms. (a) dTe time development, (b) Te-profile and (c) dTe at various times

The first core Te collapse at $t=2510.5$ ms in Figure 7(d) is similar to the H-mode recovery case as shown in Figure 4(b,d). The details of first collapse are shown in Figure 8. The small Te perturbations appearing at HFS and LFS at the startup arrive at the axis at $t=2510.5$ ms [Figure 8 (d)], similar to the case in the section 3, but in the second crash at $t=2542$ ms, no trigger cooling spot at the LFS seemed visible and the crash started only at HFS persisted and drifted toward into the LFS. This situation became more clear with the crash of third cycle at $t=2582$ ms and fourth cycle at $t=2622$ ms. These crashes show that the radial extension of Te collapse is now connected beyond $\rho \sim 0.4$

Figure 9 shows how the $n=1$ and the $n=2$ responses at off-axis extend inward to the $\rho=0.4$ domain, reaching the boundary of helical- q unity region, $\rho=0.4$, where interacts with the QI-driven core crash (Fig.9(a)). The $n=1$ reconstructed response (Fig. 9(b)) becomes maximum around $\rho=0.65$ corresponding to the $2/1$ surface and extends radially inward with a nearly constant amplitude and sharply decay around $\rho=0.4$ helical- q unity area. The $n=2$ component amplitude (Fig.9(c)) increases both at slightly-outer/inner sides of $q=2/1$ area with the variation at $2/1$ minimum as if the $n=2$ structure deforms by the even-flattening, at same time with smooth radial-extension toward $\rho=0.4$ with constant amplitude, similar to the $n=1$ behavior toward the $\rho=0.4$. The $3/2$ resonant-type response is

visible at $q=3/2$ around $\rho=0.52$. The $n=1$ and $n=2$ components are in the same magnitude $\sim 0.1\text{keV}$, significant by considering the overall δTe is $\sim 0.3\text{keV}$. The handshaking around $\rho=0.4$ takes place in the very stable manner. The further increase of the $n=1$ and $n=2$ component later in time eventually causes a minor collapse, but taking place outside the $\rho=0.4$, while the perturbation inside of $\rho=0.4$ remains minimum (detail discussion in a separate paper).

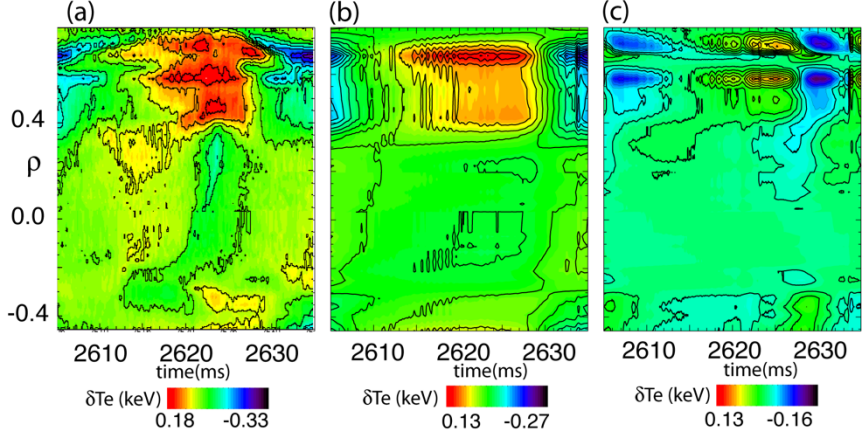


Fig. 9. The *QI-driven crash hand-shaking* with outer $n=1$ and $n=2$ reconstructed components. (a) the δTe contour by ECE profile, the reconstructed (b) $n=1$ component and (c) the $n=2$ component.

5. DISCUSSION

Slowly rotating 3D fields have been considered as a promising approach for locking avoidance and H-mode recovery against NTM-driven disruptions. This 3D field application approach has been found effective, but, near the operational limit, the application is not always successful. Recently, M3D numerical simulations[3] of locking-avoidance experiment discharge suggest there exists an additional MHD advantage of the rotating 3D field for sustaining the off-axis domain separated from the quasi-interchange. The preliminary experimental observations in the hybrid configuration discharge suggest that it may be possible to control the quasi-interchange mode stability together with the NTM-driven disruptive mode using separate aspects of the same slowly-rotating 3D field by considering the coupling between $n=1$ and $n=2$ components. Based on the core Te collapse evolution and the fluctuation behavior measured by ECE, we tentatively conclude that the QI sawtooth seen in the simulation is consistent with experimental observations and that the experimentally observed stability appears to follow the multiple criteria identified in the simulation paper, although the complete picture of QI-driven stability also depends on many other factors. Some interesting remarks and uncertainties are summarized here.

- (1) Measured behavior of the Te collapse is qualitatively consistent with the QI-driven crash seen in the simulation.
- (2) Timing of the Te(0) crash is independent of the phase of the rotating RMP phase for i-coil frequencies up to 200 Hz. The feedback of the RMP reduced the frequency of the repetitive crashes to the 30 Hz level.

The experimental observation is qualitatively consistent with the QI-type crash seen in the simulation, despite the different plasma conditions between two cases, which are listed as follows. Here, we use the shot number as the identifier: simulation (166564) and the present experiment (153967 and 153974).

- (1) Profile shape. Discharge 166564 was completely sawtooth stable because the actual central pressure profile was hollow (Te was hollow and the density profile slightly hollow over $q<1$), yielding an effective negative poloidal β_p for 1/1 mode stability (instability requires $\beta_p > \beta_{p,\text{crit}} > 0$ where β_p is a poloidal beta defined by the average of pressure gradient inside the $q=1$ surface and $\beta_{p,\text{crit}}$ is the critical value for the stability[7] while 153967 had centrally peaked density and temperature. The simulation used the slightly peaked pressure profile from the experimental EFIT

- (2) Plasma shaping. The plasmas had different flux surface shapes that increased the interchange stability (of the magnetic well parameter) of 166564 compared to 153967. The simulation shot, 166564 was a D-shaped ITER baseline plasma that scales to a 20 keV ITER burning state. Interior flux surfaces had ellipticity combined with significant triangularity, which has a stabilizing effect on the $n=1$ interchange modes [8]. The shot reported here (153967) was elliptical, with little triangularity, corresponding to greater interchange instability.

- (3) Plasma beta: 166564 had higher beta ($\beta_N=2.3$ compared to 1.5 in 153967) and a larger Shafranov shift of the magnetic axis, which increases the stabilization due to triangularity in the interchange magnetic well criterion.

Since triangularity is stabilizing for most MHD modes, 153967 is generally more unstable than the simulation shot 166564.

In summary, we have started to extend the application of an $n=1$ rotating 3D field for mode-locking avoidance to the control of the core QI-driven crash at the hybrid configuration $q \approx 1$ as well. The quasi-interchange stability in hybrid regimes with central $q \approx 1$ has dual low toroidal harmonics $n=1, 2$ that make its spectrum well suited to interact with an external 3D field. This is very helpful to integrate the MHD understanding from the core to the edge, in particular, in higher temperature less-collisional regime. The extended approach to control from core to the off-axis should contribute to develop paths attractive for successful realization of fusion reactors.

ACKNOWLEDGEMENTS

This material is based upon work supported by the U.S. Department of Energy, Office of Science, Office of Fusion Energy Sciences, using the DIII-D National Fusion Facility, a DOE Office of Science user facility, under Award(s) DE-AC02-09CH11466, DE-FC02-04ER54698, DE-AC05-06OR23100, DE-FG02-04ER54761, DE-AC52-07NA27344 and DE-SC-0017992. **Disclaimer:** This report was prepared as an account of work sponsored by an agency of the United States Government. Neither the United States Government nor any agency thereof, nor any of their employees, makes any warranty, express or implied, or assumes any legal liability or responsibility for the accuracy, completeness, or usefulness of any information, apparatus, product, or process disclosed, or represents that its use would not infringe privately owned rights. Reference herein to any specific commercial product, process, or service by trade name, trademark, manufacturer, or otherwise does not necessarily constitute or imply its endorsement, recommendation, or favoring by the United States Government or any agency thereof. The views and opinions of authors expressed herein do not necessarily state or reflect those of the United States Government or any agency thereof.

REFERENCES

- [1] PARK, W., BELOVA, E.V., FU, G.Y., TANG, X.Z., STRAUSS, H.R., AND SUGIYAMA, L.E., Phys. Plasmas 6, 1796 (1999). Plasma simulation studies using multilevel physics models
- [2] SUGIYAMA, L.E AND PARK, W., A nonlinear two-fluid model for toroidal plasmas, Phys. Plasmas 7, 4644 (2000).
- [3] SUGIYAMA, L.E., XU, L.Q., AND OKABAYASHI, M [Phys. of Plasmas submitted 2020] Quasi-interchange modes and the sawtooth crash
- [4] OKABAYASHI, M., ZANCA, P., STRAIT, E.J., GAROFALO, A.M., HANSON, J.M., IN, Y., LA HAYE, R.J., MARRELLI, L., MARTIN, P., PACCAGNELLA, R., Avoidance of tearing mode locking with electro-magnetic torque introduced by feedback-based mode rotation control in DIII-D and RFX-mod, Nucl. Fusion 57 (2017) 016035
- [5] ZANCA, P., MARRELLI, L., MANDUCHI, G., AND MARCHIORI, G., Beyond the intelligent shell concept: the clean-mode-control, Nucl. Fusion 47 (2007) 1425–1436
- [6] SHIRAKI, D., OLOFSSON, K.E.J., VOLPE, F.A., LA HAYE, R.J., STRAIT, E.J., PAZ-SOLDAN, C., AND LOGAN, N., Error Field Detection and Mode Locking Avoidance by the Interaction of Applied Rotating 3D Fields with Otherwise Locked Modes, <http://meetings.aps.org/Meeting/DPP13/Session/PO4.15>
- [7] BUSSAC, M.N., PELLAT, R., EDERY, D., SOULE, J.L., Internal Kink Modes in Toroidal Plasmas with Circular Cross Sections, Phys. Rev. Lett. 35, 1638 (1975).
- [8] GREENE, J.M., A brief review of magnetic well, Comments Plasma Phys. Controlled Fusion 17, 389 (1997). GA-A22135, April 1998.